Journal of the European Ceramic Society xxx (2016) xxx–xxx

Contents lists available at www.sciencedirect.com

Journal of the European Ceramic Society

journal homepage: www.elsevier.com/locate/jeurceramsoc

Calcium-magnesium-alumina-silicate (CMAS) resistance characteristics of $LnPO_4$ (Ln = Nd, Sm, Gd) thermal barrier oxides

Feng Wang[a,b], Lei Guo[a,b,c,*], Caimei Wang[a,b], Fuxing Ye[a,b,c,*]

[a] School of Materials Science and Engineering, Tianjin University, China
[b] Tianjin Key Laboratory of Advanced Joining Technology, Tianjin University, China
[c] Key Lab of Advanced Ceramics and Machining Technology of Ministry of Education, Tianjin University, No. 92, Weijin Road, Tianjin 300072, China

ARTICLE INFO

Article history:
Received 3 July 2016
Received in revised form 9 August 2016
Accepted 11 August 2016
Available online xxx

Keyword:
Rare-earth phosphates
Thermal barrier coatings (TBCs)
Calcium-magnesium-alumina-silicate (CMAS)
Apatite

ABSTRACT

Calcium-magnesium-alumina-silicate (CMAS) attack has been considered as a significant failure mechanism for thermal barrier coatings (TBCs). As a promising series of TBC candidates, rare-earth phosphates have attracted increasing attention. This work evaluated the resistance characteristics of $LnPO_4$ (Ln = Nd, Sm, Gd) compounds to CMAS attack at 1250 °C. Due to the chemical reaction between molten CMAS and $LnPO_4$, a dense, crack-free reaction layer, mainly composed of $Ca_3Ln_7(PO_4)(SiO_4)_5O_2$ apatite, $CaAl_2Si_2O_8$ and $MgAl_2O_4$, was formed on the surface of compounds, which had positive effect on suppressing CMAS infiltration. The depth of CMAS penetration in $LnPO_4$ (Ln = Nd, Sm, Gd) decreased in the sequence of $NdPO_4$, $SmPO_4$ and $GdPO_4$. $GdPO_4$ had the best resistance characteristics to CMAS attack among the three compounds. The related mechanism was discussed based on the formation ability of apatite phase caused by the reaction between molten CMAS and $LnPO_4$.

1. Introduction

Thermal barrier coatings (TBCs) are widely applied on the hot section components of gas turbine, aiming at increasing engine's operating temperature and durability [1–3]. A TBC system is typically composed of a metallic bond coat and a ceramic top coat. The bond coat protects the substrate from corrosion and oxidation and improves the adhesion between ceramic top coat and substrate [4–6]. The ceramic top coat acts as a thermal insulation layer, and it is usually made of yttria stabilized zirconia (YSZ). TBCs can be produced by various methods, including plasma spraying (PS), electron beam physical vapor deposition (EB-PVD), plasma spray physical vapor deposition (PS-PVD) [7–11]. The failure behaviors of YSZ TBCs were investigated, and many mechanisms have been proposed. Recently, damage from calcium-magnesium-alumina-silicate (CMAS) is becoming a critical issue for TBCs due to the rising engine's temperature. Detailed analysis of the CMAS related damage to YSZ TBCs has been investigated [12–16]. There appears to be an urgent need to develop approaches to protect TBCs from CMAS attack.

In open literatures, many reports on improving TBCs' resistance to CMAS attack can be found. Sohn et al. fabricated dense, crack-free alumina overlay for YSZ TBCs by electrophoretic deposition. They have pointed out that the overlay can suppress the infiltration of CMAS to YSZ coatings [17]. Zhang et al. first deposited Al film on the surface of YSZ TBC by magnetron sputtering followed by vacuum heat treatment, and the samples exhibit better CMAS corrosion resistance [18]. Rai et al. produced a Pd film on YSZ surface by magnetron sputtering, and the sample was isothermal treatment to obtain crack-free, reglazed Pd coating [19]. They have found that the Pd coating can protect YSZ coating from CMAS attack effectively. Guo et al. have deposited a dense and defect-free Pt film on YSZ coating surface by EB-PVD and found it can provide effective protection from CMAS attack [20]. It has been reported that doping 20 mol% Al_2O_3 and 5 mol% TiO_2 to YSZ coating can significantly improve its resistance to CMAS attack [21–23]. Padture et al. have fabricated YSZ TBCs containing Al^{3+} and Ti^{4+} in solid solution by APS and found it has high resistance to CMAS attack [24].

Apart from modifying YSZ to obtain better CMAS resistance characteristics, alternate materials to YSZ have been developed. Rare-earth zirconates ($Ln_2Zr_2O_7$, Ln = rare earth element) have been proposed as a promising series of TBC candidates [25–27]. They have low thermal conductivity, excellent phase stability and desirable high temperature capability. It has been reported that $Ln_2Zr_2O_7$ coatings have excellent CMAS resistance [28,29]. In CMAS conditions, $Ln_2Zr_2O_7$ could react with molten CMAS to form a seal-

* Corresponding authors at: School of Materials Science and Engineering, Tianjin University, China.
E-mail addresses: glei028@tju.edu.cn, glei028@163.com (L. Guo), yefx@tju.edu.cn (F. Ye).

http://dx.doi.org/10.1016/j.jeurceramsoc.2016.08.013
0955-2219/

ing layer rapidly. The layer mainly consist of an apatite phase based on $Ln_8Ca_2(SiO_4)_6O_2$. As a result, CMAS infiltration in the coating can be arrested. Besides, another TBC candidate, $La_2Ce_2O_7$, has also been reported to have excellent performance of resisting CMAS attack. The related mechanism has been clarified by Guo et al. They have pointed out that the key factor is the formation of a reaction layer consisting of $Ca_2(La_xCe_{1-x})_8(SiO_4)_6O_{6-4x}$ and CeO_2 [30]. Wang et al. fabricated several rare earth disilicates ($Ln_2Si_2O_7$, Ln = rare earth element), and analyzed their CMAS corrosion behaviors. The results have indicated that $Ln_2Si_2O_7$ could react with CMAS in the temperature range of 1250–1350 °C, and the reaction layer can inhibit CMAS further infiltration [31]. It has been reported that the penetration of molten CAMS in $LaMgAl_{11}O_{19}$ compound can be arrested due to the formation of a reaction layer [32].

Lanthanum phosphate ($LaPO_4$) has high-temperature stability, low thermal conductivity and high thermal expansion. Importantly, $LaPO_4$ is found to be compatible with Al_2O_3, which is the main constitution of thermally grown oxide (TGO) formed on the metallic bond coat under oxidative conditions typical of operation [33–35]. Therefore, $LaPO_4$ is viewed as a promising TBC candidate, and have attracted increasing attention. Since rare-earth phosphates ($LnPO_4$, Ln = rare earth element) have similar structure, they are considered to have similar chemical and physical properties. Hence, $LnPO_4$ might be a series of materials suitable for TBC application. However, limited report on the CMAS corrosion behavior of this type of materials can be found. In this study, several rare-earth phosphates ($NdPO_4$, $SmPO_4$ and $GdPO_4$) were fabricated, and the compounds were exposed to CMAS deposits at 1250 °C. Investigations were focused on the microstructure variation of these compounds due to CMAS attack. The resistance characteristics of these compounds to CMAS attack were compared, and the related mechanisms were discussed. For comparison, the CMAS corrosion behavior of YSZ was also studied.

2. Experimental procedure

$LnPO_4$ (Ln = Nd, Sm, Gd) powders were synthesized by a chemical route using 99.99% pure Ln_2O_3 (Ln = Nd, Sm, Gd) and *ortho*-phosphoric acid (85%) as the raw materials. Ln_2O_3 (Ln = Nd, Sm, Gd) and phosphoric acid were taken in appropriate proportion. Phosphoric acid was diluted with equal volume of water and then Ln_2O_3 (Ln = Nd, Sm, Gd) powders were dissolved in it. The chemical reaction equation of phosphoric acid and Ln_2O_3 is presented as follow:

$$Ln_2O_3 + 2H_3PO_4 \rightarrow 2LnPO_4 + 3H_2O \quad (1)$$

In order to ensure complete conversion of the oxide to phosphate, phosphoric acid was taken in excess. To make reaction solution homogeneous, mechanical agitation was carried out for 15 min. Subsequently, the solution was filtered and washed with distilled water and alcohol several times. The obtained precipitates were dried at 120 °C for 5 h and then calcined at 800 °C for 5 h to crystallize. The calcined powders were cold pressed at ~300 MPa and then sintered at 1600 °C to obtain bulks. The acquired bulks were ground using 400, 800, 1200, 1500 and 2000 grit SiC abrasive papers followed by polishing for 10 min. YSZ bulk was also prepared for comparison.

CMAS with a composition of 22CaO-19MgO-15$AlO_{1.5}$-44SiO_2 in mole ratio was used in this study. All these raw materials were weighted in the molar ratio and suspended in deionized water. The mixture was fully mixed by planetary ball milling (QM-3SP4) with absolute alcohol for 5 h at a speed of 400 rpm. The suspension was dried at 120 °C for 6 h. The obtained CMAS powders were dissolved in absolute alcohol and fully stirred. The homogeneous suspension was dropped on the surfaces of $LnPO_4$ (Ln = Nd, Sm, Gd) bulks with a concentration of about 15 mg/cm^2. After the evaporation of alcohol, CMAS powder was evenly deposited on the surface of bulk. The $LnPO_4$ (Ln = Nd, Sm, Gd) bulks with CMAS deposits were heat-treated in box electric furnace (SX-1600 °C) at 1250 °C for 4 h.

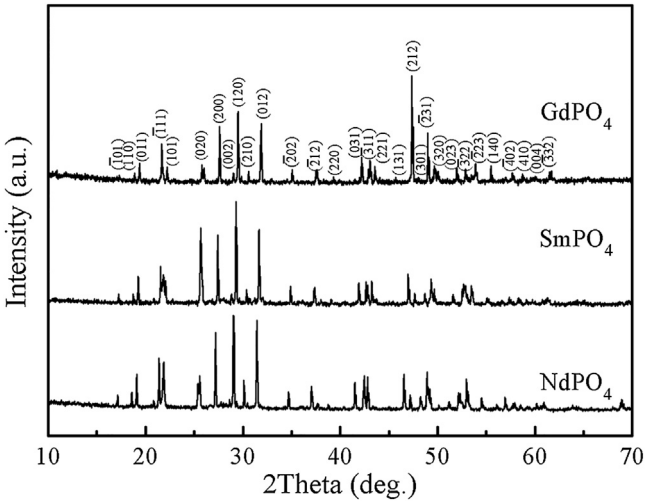

Fig. 1. XRD patterns of $LnPO_4$ (Ln = Nd, Sm, Gd) bulks.

Phase composition was characterized by an X-ray diffraction (XRD, Bruker D8 Advanced, Germany) using CuKα radiation. Data were digitally recorded in a continuous scan in the range of angle (2θ) from 10° to 70° with a scanning rate of 0.1°/s. The cross section morphologies of the CMAS attacked samples were examined by a scanning electron microscopy (SEM, SU1510, Japan). Transmission electron microscopy (TEM) specimens from CMAS attacked bulks were prepared using a focused ion beam (FIB) and the morphologies were observed by a transmission electron microscope (TEM, JEM-2100, Japan) equipped with energy dispersive spectrum (EDS).

3. Results and discussion

Fig. 1 shows the XRD patterns of $LnPO_4$ (Ln = Nd, Sm, Gd) bulks. The three XRD patterns exhibit similar appearance. $LnPO_4$ bulks consist of a single homogeneous phase, with a monazite structure. By comparing these three XRD patterns, a slight shift in the diffraction peaks can be observed, indicating the difference in the lattice parameter. Since $LnPO_4$ (Ln = Nd, Sm, Gd) have similar crystal structure, the different lattice parameter of each compound could be attributed to the different ionic radii of Nd^{3+}, Sm^{3+} and Gd^{3+}. The ionic radii of Nd^{3+}, Sm^{3+} and Gd^{3+} in 8-fold coordination are 1.109 Å, 1.079 Å and 1.053 Å, respectively [36]. Thus, the lattice parameters of $LnPO_4$ (Ln = Nd, Sm, Gd) decrease in the sequence of $NdPO_4$, $SmPO_4$ and $GdPO_4$. As a result, $GdPO_4$ has diffraction peaks at the highest angles among the three compounds.

CMAS powders were deposited on the surfaces of $LnPO_4$ (Ln = Nd, Sm, Gd) bulks. The CMAS covered samples were annealed at 1250 °C for 4 h. YSZ bulk was treated in the same way for comparison. The digital photographs of the samples after CMAS attack are shown in Fig. 2. It appears that molten CMAS spreads uniformly on the surface of YSZ bulk, while many droplets are found on the surfaces of $LnPO_4$ (Ln = Nd, Sm, Gd) bulks, suggesting that the surface tension of the CMAS on $LnPO_4$ is larger and thus prevents it from undergoing substantial wetting effectively. These observations indicate that $LnPO_4$ have better non-wetting characteristics toward CMAS than YSZ. As a result, the molten CMAS's ability to penetrate $LnPO_4$ is weaker, which might contribute to better CMAS resistance of the compound.

Fig. 3 shows the XRD patterns of $LnPO_4$ (Ln = Nd, Sm, Gd) bulks exposed to CMAS deposits at 1250 °C for 4 h. All the XRD

Please cite this article in press as: F. Wang, et al., Calcium-magnesium-alumina-silicate (CMAS) resistance characteristics of $LnPO_4$ (Ln = Nd, Sm, Gd) thermal barrier oxides, *J Eur Ceram Soc* (2016), http://dx.doi.org/10.1016/j.jeurceramsoc.2016.08.013